

THE PACIFIC INFRASOUND EVENT OF APRIL 23, 2001

David J. Brown¹, Anna K. Gault¹, Riley Geary¹, Pierre Caron¹, and Relu Burlacu²

Science Applications International Corporation (SAIC)¹
Mission Research Corporation²

Sponsored by Defense Threat Reduction Agency

Contract No. DTRA01-99-C-0025

ABSTRACT

For the past several years, the Defense Threat Reduction Agency's (DTRA) Center for Monitoring Research (CMR) in Arlington, Virginia, has been developing and testing software to extend the International Data Centre nuclear explosion monitoring system to include infrasound monitoring of the atmosphere. This system can form infrasound-only events, or form fused events using any combination of infrasound, seismic, and hydroacoustic data. Evaluation of the performance of the infrasound processing system is hampered by the scarcity of major infrasound events.

On April 23, 200, a significant infrasound event occurred, providing a good test case for the system. Signals from this event, subsequently confirmed by optical observations to be a bolide impact over the Northern Pacific Ocean, were recorded on a number of infrasonic arrays in North America and Hawaii. Using arrival information from several International Monitoring System (IMS) infrasound arrays, an acoustic-only event was built automatically as part of standard event processing at the Prototype International Data Center (PIDC). After optical confirmation it was determined that the infrasound and optical locations differed by 3 minutes in origin time and 80 km in location, which is within the estimated error of the infrasound location. This paper presents the Prototype IDC analysis of this event and the subsequent studies undertaken at CMR to refine the hypothesized source location and evaluate the infrasound processing system.

A number of signal characteristics, such as duration and dominant period, make the April 23 event significant for evaluating nuclear explosion monitoring capability. To provide a better understanding of what characteristics constitute significant signals and to provide a better discrimination capability, CMR has been compiling a collection of infrasonic signals that, for various reasons, are considered to be noteworthy. This infrasound waveform library is being made accessible to researchers for independent research by the CMR Research and Development Support System (RDSS). The infrasound library is divided into several subsections that include a ground-truth database, the ENSCO collection compiled by the University of Alaska, as well as a collection of synthetic-signal data. A web-based interface has been developed to allow easy access to the waveforms. This paper provides a summary of the waveform library and how it may be accessed.

KEY WORDS: infrasound, infrasonic event, infrasound waveform library.

OBJECTIVE

The objective of this research is to improve the current infrasound source location and discrimination capability of the fused seismic-hydroacoustic-infrasound-radionuclide data processing system being developed at the CMR. The occurrence in the last 12 months of two large bolide (meteorite) events with acoustic signals that were recorded on numerous IMS-style infrasound arrays, provides an opportunity to gauge performance of the automatic infrasound detection and source location system, as well as an opportunity for system refinement. In this investigation, various velocity models will be used with acoustic arrival information from each of the bolide events, in conjunction with a nonlinear source location procedure to determine the merits of each velocity model.

During event analysis, various characteristics of the recorded waveforms suggested that these events were significant from a monitoring perspective. However, the infrasound source characterization and discrimination procedures are still rudimentary and at an early stage of development. As an aid to improving discrimination, and automatic detector design, developmental work on an infrasound waveform library has commenced at CMR as part of the RDSS. This data collection will be invaluable to independent researchers and is being made available to the research community via a web-based interface.

RESEARCH ACCOMPLISHED

Optical source location information as provided by Los Alamos National Laboratory (LANL, 2001a; LANL, 2001b) for the two bolide events considered in this investigation are listed in Table 1.

Table 1: Bolide events considered in the present study.

| Name | Lat | Lon | Time | Energy (J) |
|---------------|-------|---------|---------------------|----------------------|
| Acapulco | 14.45 | -106.13 | 2000/08/25 01:12:25 | 1.4×10^{12} |
| North Pacific | 27.90 | -133.89 | 2001/04/23 06:12:35 | 4.6×10^{12} |

In what follows, each bolide event will be considered independently.

Acapulco Event

Location information for the recording arrays for this event are shown in Table 2 as well as source to receiver backazimuth, θ , and distance, Δ , along the great-circle.

Table 2: Geographical information for the recording arrays.

| Station | Lat | Lon | Location | θ (deg) | Δ (km) |
|---------|---------|-----------|-----------------------------|-------------------|------------------|
| DLIAR | 35.8667 | -106.3342 | Los Alamos, New Mexico, USA | 179.5 | 2381 |
| ISS9 | 19.5917 | -155.8934 | Hawaii, USA | 88.0 | 5304 |

Arrival information for the IMS-style arrays for this event are shown in Table 3. Azimuth variances, $\delta\theta$, of around 2.5 degrees were found for both stations. A time variance, δT , of 5 sec were used for both stations as this corresponds approximately to one wave period. This value for δT may be too small and the effect on source location of larger values needs to be investigated.

Table 3: Arrival information for the IMS-style recording arrays for the Acapulco Event.

| Station | Observed Signal Time T | δT (sec) | Arrival Azimuth θ (deg) | $\delta\theta$ (deg) | F-stat | Signal Duration (min) | Dom. Freq. (Hz) |
|---------|------------------------|------------------|--------------------------------|----------------------|--------|-----------------------|-----------------|
| DLIAR | 2000/08/25 03:28:52 | 5.0 | 181.3 | 2.5 | 21 | 11.4 | 0.20 |
| IS59 | 2001/08/25 06:05:27 | 5.0 | 89.2 | 2.5 | 43 | 18.3 | 0.17 |

Although the signal from this event was automatically detected at the DLIAR array, maintenance work prevented automatic detection at the IS59 array. An automatic source location was therefore never formed. Subsequent analysis, however, was performed.

Following Jordan and Sverdrup (1981), and Bratt and Bache (1988), a least-squares inversion procedure was applied to the arrival information contained in Table 3. Both azimuth and time were made ‘defining’ for this algorithm, but slowness was set as ‘un-defining’ so that it played no role in the source location procedure.

Travel-time information for these location exercises was provided by one of two different methods. The first uses travel-time information assigned via travel time-tables generated using a seasonal propagation model (based on the MSISE-90 temperature model of Hedin, (1991), and the HWM-93 wind model of Hedin et al., (1996)), and the second assumes a constant average horizontal signal propagation speed. Several different propagation speeds were used. The following variances were assumed for the respective travel-time models where s is distance in km:

$$\Delta T = 1462\sqrt{s/10000} \quad (\text{sec}) \quad \text{Constant velocity model appropriate for stratospheric signals.}$$

$$\Delta T = \begin{cases} 1800\frac{s}{2500} & ; s < 2500 \\ 1800 + (7200 - 18000)\left(\frac{s - 2500}{21000 - 2500}\right) & ; s > 2500 \end{cases} \quad (\text{sec}) \quad \text{Seasonal model}$$

Although large, the variances for the seasonal model were designed to accommodate the possible phase mis-identification when stratospheric phases were assigned thermospheric travel-times or vice-versa.

Observed and seasonally-predicted values for the average horizontal velocity, V , are shown for each array in Table 4. Clearly, thermospheric travel-times are predicted for the signals at DLIAR and stratospheric travel-times for the signals at IS59. This is significantly what one would expect for the particular season and geographic location of the arrays. In the summer, the stratospheric winds will be predominantly toward the west, strongly influencing the signal at IS59. The azimuth of arrival at DLIAR, however, is directed largely toward the north and so the signals will not benefit from the seasonal stratospheric winds. The observed average horizontal velocity at each array, of course, implies stratospheric signals at each array.

Table 4: Observed and predicted average horizontal velocities.

| Sta | V (observed) | V (predicted) |
|-------|--------------|---------------|
| DLIAR | 291 | 253 |
| IS59 | 302 | 313 |

Shown in Table 5 are the hypothesized source locations for various velocity models. Also shown are the spatial and temporal mislocations and size of the 90% confidence ellipse for each model.

Table 5: 90% confidence source location results for various velocity models. Model number indicates constant velocity (in m/s) used. Semi-major axis is indicated by Smaj, Semi-minor axis is indicated by Smin.

| Model | Lat | Lon | Time | Spatial mislocation Δ (km) | Temporal mislocation ΔT (min) | Smaj (km) | Smin (km) |
|--------|------|--------|-------|-----------------------------------|---------------------------------------|-----------|-----------|
| 290 | 13.6 | -106.9 | 01:05 | 124 | 7 | 387 | 195 |
| 295 | 13.7 | -106.9 | 01:09 | 116 | 3 | 162 | 82 |
| 300 | 13.8 | -106.8 | 01:12 | 107 | 0 | 58 | 29 |
| summer | 14.7 | -106.6 | 01:04 | 62 | 8 | 2606 | 1294 |

The constant velocity source locations have clearly benefited from phase identification where a substantially refined variance for the travel-times was possible. The apparent improvement in spatial mislocation in the case of the seasonal model is simply a manifestation of the fact that large variances on the travel-times were used, and only two stations were used to form the source location. In such a case, the source location algorithm will tend to locate the source at the great-circle intersection as defined by the backazimuth at each array. A representative example of the signals recorded from this event (IS59) is shown in Figure 1.

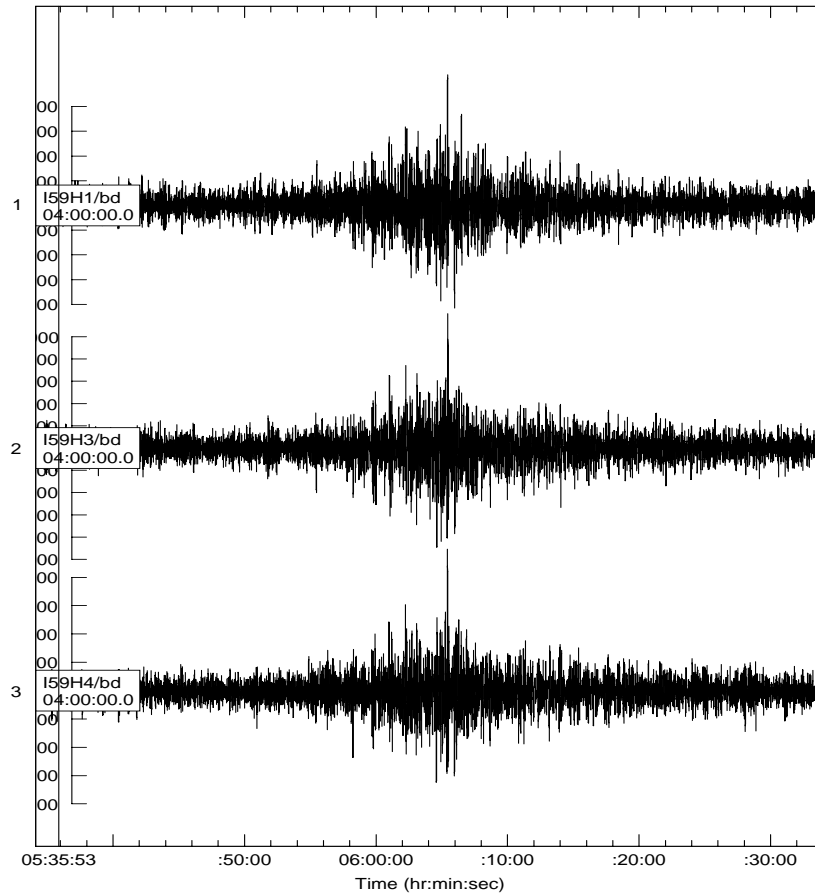


Figure 1: Signal recorded at IS59 (Hawaii) - 5304 km from the Acapulco event. No data were available for channel H2. Time is UTC.

North Pacific Event

This event was formed automatically at the CMR using detections on two IMS infrasound arrays. The Hawaii array (IS59) and the Lac du Bonnet, Manitoba array (IS10) were the closest IMS arrays contributing to standard event formation at the time of the event, and detections from these arrays were used to build the event in the Standard Event List 3 (SEL3). The signal was also detected at a number of other infrasound arrays. The most distant station to record the signal is located in Freyung, Germany (IS26), 10800 km from the estimated source location. The Pinon Flat array, California (IS57), Windless Bight, Antarctic array (IS55), and the IMS prototype array in New Mexico (DLIAR) operated by LANL, were not transmitting data to the PIDC at the time of the event. IS55 and IS57 are newly installed arrays and at the time of the event were not providing data feeds for all PIDC processing. Data from both the DLIAR array and IS57 array were later recovered and transmitted to the PIDC.

Location information for the recording arrays for this event are shown in Table 6 as well as source to receiver backazimuth, θ , and distance, Δ , along the great-circle.

Table 6: Geographical information for the recording arrays.

| Station | Lat | Lon | Location | θ (deg) | Δ (km) |
|---------|---------|-----------|-----------------------------|-------------------|------------------|
| IS57 | 33.6056 | -116.4544 | Pinon Flat, California, USA | 253.9 | 1781 |
| NVIAR | 38.4295 | -118.3037 | Nevada, USA | 235.7 | 1836 |
| IS59 | 19.5917 | -155.8934 | Hawaii, USA | 63.5 | 2408 |
| DLIAR | 35.8667 | -106.3342 | Los Alamos, New Mexico, USA | 259.0 | 2737 |
| IS10 | 50.2010 | -96.0270 | Winnipeg, Canada | 246.5 | 4002 |
| IS26 | 48.8516 | 13.7131 | Freyung, Germany | 331.4 | 10837 |

Arrival information for these stations is shown in Table 7.

Table 7: Arrival information for the bolide of 2001/04/23.

| Station | Observed Signal Time T | δT (sec) | Arrival Azimuth θ (deg) | $\delta\theta$ (deg) | F-stat | Signal Duration (min) | Dom. Freq. (Hz) |
|---------|------------------------------|---------------------|--------------------------------------|-------------------------|--------|-----------------------------|-----------------------|
| IS57 | 2001/04/23 07:51:48 | 5.0 | 254.7 | 3.00 | 290 | 11.5 | 0.25 |
| NVIAR | 2001/07/23 07:56:25 | 5.0 | 239.7 | 2.02 | 35 | 7.0 | 0.22 |
| IS59 | 2001/07/23 08:28:05 | 5.0 | 62.4 | 2.05 | 43 | 15.8 | 0.25 |
| DLIAR | 2001/07/23 08:44:51 | 5.0 | 261.9 | 2.00 | 81 | 13.8 | 0.24 |
| IS10 | 2001/07/23 09:58:52 | 5.0 | 244.4 | 2.50 | 128 | 15.5 | 0.21 |
| IS26 | 2001/07/23 16:26:28 | 5.0 | 324.9 | 2.00 | 27 | 8.0 | 0.15 |

A representative example of the signals recorded from this event (IS57) is shown in Figure 2.

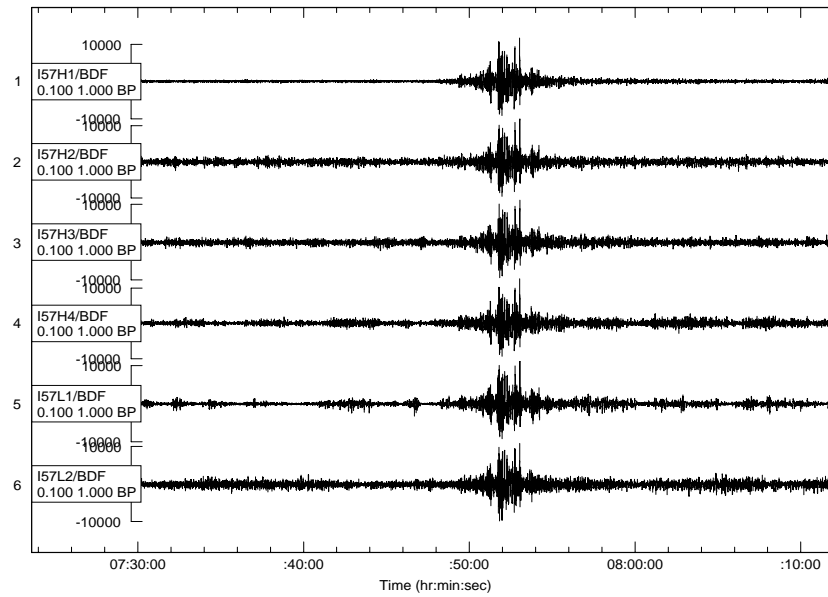


Figure 2: Signal recorded at IS57 (Pinon Flat, California) - 1781 km from the North Pacific event. No data were available for channels L3 and L4, as the station was not yet fully installed. Time is in UTC

Observed and seasonally-predicted values for the average horizontal velocity, V , are shown for each array in Table 8.

Table 8: Observed and predicted average horizontal velocities.

| Sta | V (observed) | V (predicted) |
|-------|--------------|---------------|
| IS10 | 295 | 273 |
| IS26 | 294 | 292 |
| IS57 | 299 | 265 |
| IS59 | 296 | 262 |
| DLIAR | 300 | 256 |
| NVIAR | 295 | 270 |

The seasonal model clearly predicts thermospheric arrivals at all stations, except IS26. This is completely consistent with the time of year and geographical location of the stations. In the northern hemisphere, strong stratospheric winds from the east are associated with the summer months, and strong stratospheric winds from the west are associated with the winter months. April, in between, is representative of the change of seasons, with generally weak to non-existent stratospheric winds and predominant thermospheric returns. However, for this event, observed horizontal velocities indicate stratospheric arrivals at all stations. The constant velocity source locations as indicated in Table 9 show smaller mislocations and confidence ellipses, as one would expect since the constant velocity travel-times were developed preferentially favoring stratospheric signals. The azimuth and time residuals shown in Table 10 also favor the constant velocity model, as one would expect.

Table 9: 90% confidence source location results for various velocity models. Model number indicates constant velocity (in m/s) used. Semi-major axis is indicated by Smaj, Semi-minor axis is indicated by Smin.

| model | lat | lon | Time | Spatial mislocation Δ (km) | Temporal mislocation ΔT (min) | Smaj (km) | Smin (km) |
|--------|------|--------|-------|---|---|--------------|--------------|
| 290 | 28.5 | -134.3 | 06:09 | 78 | -3 | 147 | 55 |
| 300 | 28.5 | -134.3 | 06:13 | 78 | 1 | 151 | 55 |
| spring | 28.5 | -134.5 | 05:55 | 90 | 17 | 177 | 61 |

Table 10: Azimuth and time residuals at each station

| station | 290 m/s | | spring | |
|---------|---------------------------|------------------------|---------------------------|------------------------|
| | azimuth residual (deg) | time residual (sec) | azimuth residual (deg) | time residual (sec) |
| IS59 | 0.9 | 47.8 | 0.8 | 10.8 |
| IS10 | -3.3 | -52.2 | -3.3 | -111.3 |
| NVIAR | 1.4 | 86.7 | 1.3 | 357.0 |
| IS57 | -1.5 | -9.7 | -1.4 | 145.2 |
| DLIAR | 1.0 | -131.2 | 1.1 | -669.6 |

The source locations for both the 290 m/s model and seasonal velocity model are indicated in Figure 3 together with the 90% confidence ellipses.

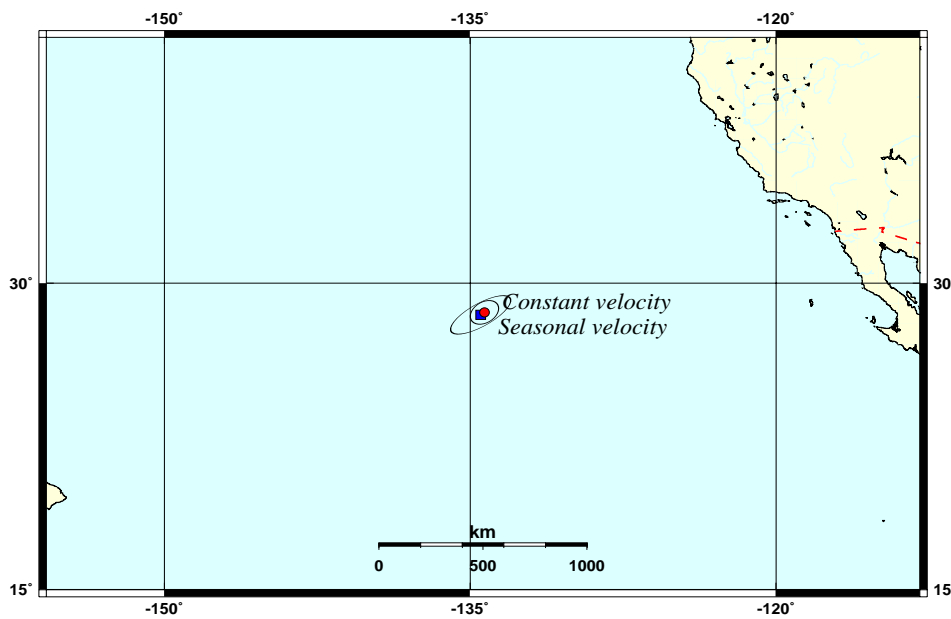


Figure 3. Source locations and 90% confidence ellipses for the 290 m/s model and seasonal velocity model.

These infrasonic source location exercises with both constant and seasonal velocity models show that the constant velocity models appear to perform better, providing smaller mislocations. This, however, should be expected since the velocity models were developed to preferentially favor stratospheric signals and knowledge of the ground-truth source information indicates stratospheric signals at each station, contrary to what one would expect based on seasonal information alone. These results strongly indicate that source location without phase identification can lead to larger than necessary mislocations and confidence ellipses.

Infrasound waveform library

Various signal characteristics were used to establish the significant nature of the Acapulco and North-Pacific events. Signal duration and dominant period are two such characteristics. To provide a better understanding of what constitutes a significant signal, and to provide a better discrimination capability, CMR has been compiling a collection of infrasonic signals that, for various reasons, are considered to be noteworthy.

The ‘Infrasound Waveform Library’ is composed of several data collections:

1. The Infrasound Ground Truth Database
2. The ENSCO infrasound waveform library compiled by the University of Alaska (Hutchenson, 1997).
3. A synthetic waveform library
4. The IDG-Russian Academy of Sciences/Maxwell collection of acoustic signals from Soviet Union Nuclear detonations, 1961 (Stevens, 2001)

When compiling the Infrasound Ground Truth Database, some attention is paid to establishing the most accurate source location. As such, each event is being assigned a ‘GT’ number that reflects the uncertainty in kilometers of the known source location. In addition, some effort is being made to trace the originator of the location information. This information is contained in a flat ascii file identified by an event number with a ‘.txt’ extension. The infrasound waveform library is being made accessible to researchers for independent research by the CMR RDSS. A web-based interface allowing researchers access to event information and signal data has been constructed. An example, taken from the Infrasound Ground Truth Database is shown in Figure 4. In this example, one chooses the appropriate GT value for the event (Screen 1) and the source type and then submits the query. All events satisfying the query are then listed in the next screen (Screen 2).



screen 1

Source Type

- ro rocket launch
- bo bolide
- ce chemical explosion
- gp gas pipe
- eq earthquake
- vo volcano

| Event | Date | Time | Lat | Lon | GT | Days | Workdays | Status |
|-------|-----------|------------|-----------|------------|------|------|----------|--------|
| 1 | 19970909 | 18:47:11.0 | 11 8000.0 | 100 3000.0 | 0719 | 1a | 1.0a | 1.0a |
| 2 | 199710 11 | 17:43:28.0 | 11 6000.0 | 100 4707.0 | 0719 | 1a | 1.0a | 1.0a |
| 3 | 199710 09 | 17:38:42.0 | 11 6000.0 | 100 4707.0 | 0719 | 1a | 1.0a | 1.0a |
| 4 | | | | | | | | |
| 5 | 19970908 | 22:44:41.0 | 11 8147.0 | 100 4700.0 | 0719 | 1a | 1.0a | 1.0a |
| 6 | 199710 07 | 15:01:30.0 | 11 6000.0 | 100 4000.0 | 0719 | 1a | 1.0a | 1.0a |
| 7 | | | | | | | | |
| 8 | 199710 11 | 11:11:30.0 | 11 6000.0 | 100 4000.0 | 0719 | 1a | 1.0a | 1.0a |
| 9 | 199710 11 | 10:20:00.0 | 11 6700.0 | 100 5200.0 | 0719 | 1a | 1.0a | 1.0a |
| 10 | 199710 11 | 09:40:00.0 | 11 7000.0 | 100 4000.0 | 0719 | 1a | 1.0a | 1.0a |
| 11 | 199710 11 | 09:17:30.0 | 11 6000.0 | 90 4000.0 | 0719 | 1a | 1.0a | 1.0a |
| 12 | 199710 11 | 07:29:20.0 | 11 6000.0 | 107 2000.0 | 0719 | 1a | 1.0a | 1.0a |
| 13 | 199710 11 | 06:40:40.0 | 11 5000.0 | 100 4000.0 | 0719 | 1a | 1.0a | 1.0a |
| 14 | 199710 09 | 18:09:40.0 | 11 3120.0 | 100 1000.0 | 0719 | 1a | 1.0a | 1.0a |
| 15 | 199710 09 | 18:47:30.0 | 11 7000.0 | 100 4000.0 | 0719 | 1a | 1.0a | 1.0a |
| 16 | 20000109 | 09:00:00.0 | 07000.0 | 100 1000.0 | 0719 | 1a | 1.0a | 1.0a |
| 17 | 20000109 | 11:20:00.0 | 11 3000.0 | 100 4000.0 | 0719 | 1a | 1.0a | 1.0a |
| 18 | | | | | | | | |
| 19 | 200010 11 | 23:17:30.0 | 11 6000.0 | 90 4000.0 | 0719 | 1a | 1.0a | 1.0a |
| 20 | 200010 07 | 22:11:30.0 | 11 6000.0 | 90 4000.0 | 0719 | 1a | 1.0a | 1.0a |
| 21 | 200010 08 | 19:34:30.0 | 11 2000.0 | 111 7000.0 | 0719 | 1a | 1.0a | 1.0a |
| 22 | 200010 08 | 18:43:30.0 | 11 6000.0 | 90 4000.0 | 0719 | 1a | 1.0a | 1.0a |
| 23 | 200001 01 | 00:22:00.0 | 11 6000.0 | 100 1000.0 | 0719 | 1a | 1.0a | 1.0a |
| 24 | 200010 07 | 20:02:00.0 | 11 6000.0 | 110 8000.0 | 0719 | 1a | 1.0a | 1.0a |
| 25 | 199710 09 | 18:00:00.0 | 11 6000.0 | 100 5200.0 | 0719 | 1a | 1.0a | 1.0a |
| 26 | 199710 07 | 15:00:00.0 | 11 6000.0 | 90 4000.0 | 0719 | 1a | 1.0a | 1.0a |

screen 2

Figure 4. Web-based interface for the Infrasound Ground Truth Data Base.

The user has the option of selecting a tar image, where data for the event resides, or displaying an image of the waveform, or learning about the originator of the location information by selecting the 'Source' column.

An example of the sort of discrimination studies possible with the Infrasound Waveform Library is shown in Figure 5. Displayed here is the dominant period versus signal duration for various sources including bolides, historical nuclear detonations, rocket launches and earthquake generated infrasonic signals. Clustering between the large impulsive detonations and less impulsive rocket-type signals is obvious.

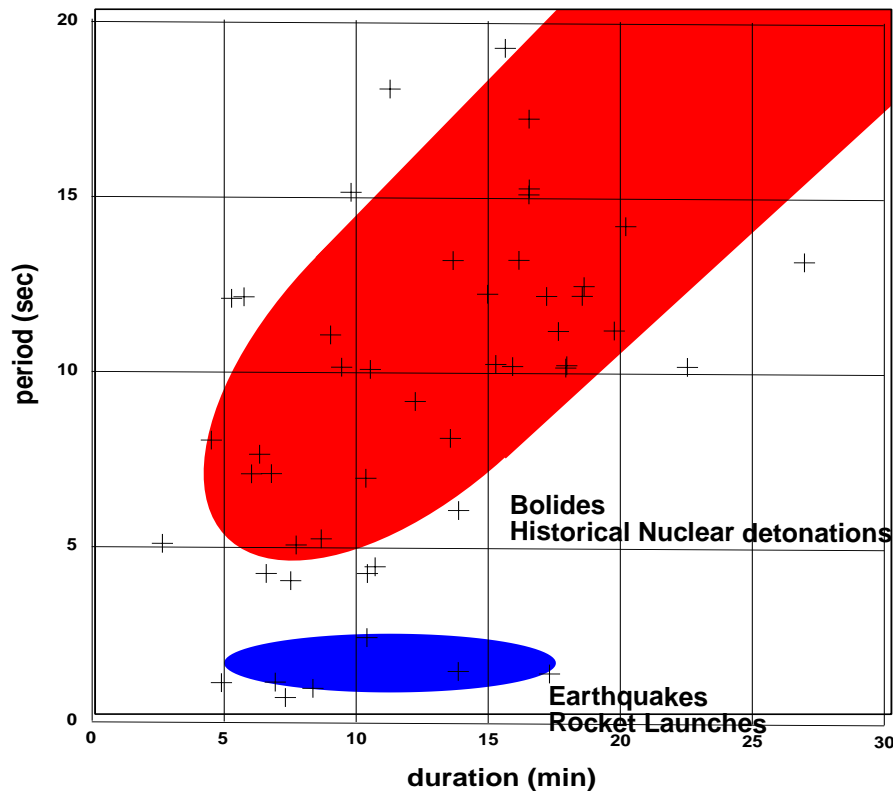


Figure 5. Signal duration versus dominant signal period for various sources. The upper shaded red area corresponds to the bolide and historical nuclear detonation signals, and the lower blue area corresponds to the earthquake and rocket launch signals.

CONCLUSIONS AND RECOMMENDATIONS

Acoustic signals from large bolides provide an excellent source of data to test and refine the detection/location capability of the developing fused seismic-infrasound-hydroacoustic-radionuclide system at the CMR. The fact that, for these two events at least, the constant velocity models yielded a better mislocation strongly suggests that phase identification is necessary in order to refine variances on travel-time information prior to source location. The fact that stratospheric arrivals were found where thermospheric arrivals were expected suggests that it may be necessary to incorporate updated meteorological data above the seasonal information to correctly predict the likely phases. The use of updated meteorological data needs to be explored further as does the extent to which local meteorology causes azimuthal deviation and thus influences source location. It is clear from the basic discrimination exercises performed here that large explosive sources generate signals with different characteristics to those of the less impulsive, but equally long duration, rocket and earthquake generated acoustic signals. These source characterization and discrimination investigations need to continue and will be enhanced by access to the CMR RDSS Infrasound Waveform Library.

REFERENCES

- Bratt, S.R., and T. C. Bache (1988), Locating Events With a Sparse Network of Regional Arrays, Bull. Seism. Soc. Am. 78, No. 2, 78-798.
- Hedin, A.E. (1991), Extension of the MSIS thermosphere model in the middle and lower atmosphere", J. Geoph. Res. 96, 1159-1172.
- Hedin, A.E., E.L. Fleming, A.H. Manson, F.J. Schmidlin, S.K. Avery, R.R. Clark, S.J. Franke, G.J. Fraser, T. Tsuda, F. Vial, and R.A. Vincent, (1996) Empirical wind model for the upper, middle and lower atmosphere, J. Atmos. Terr. Phys. 58, 1421-1444.
- Hutchenson, K. D., (1997) Acquisition of Historical Infrasonic Data. Final Technical Report. ENSCO Inc. Contract No. F08650-95-D-0033.
- Jordan, T. H, and K.A. Sverdrup.(1981), Teleseismic location techniques and their application to earthquake clusters in the South-Central Pacific. Bull. Seism. Soc. Am, 71, No 4., 1105-1130.
- LANL 2001a. Los Alamos National Laboratory, Press release, May 23, 2001.
- LANL 2001b, Los Alamos National Laboratory, Press release, May 23, 2001.
- Stevens, J. L., (2001) Infrasound Excitation and Propagation Research (Draft Report), Contract No. DSWA01-97-C-0129.